

Supporting Information

Three-dimensional porous borocarbonitride composed of pentagonal motifs as a high-performance pyroelectric material

Changsheng Hou ^a, Yiheng Shen ^a, Jiaqi, Xin ^b, Yaguang Guo ^{b,*}, and Qian Wang ^{a,*}

^a CAPT, School of Materials Science and Engineering, HEDPS, BKL-MEMD, Peking University, Beijing 100871, China. Email: qianwang2@pku.edu.cn

^b Department of Physics, School of Physical Science and Engineering, Beijing Jiaotong University, Beijing 100044, China. Email: ygguo@bjtu.edu.cn

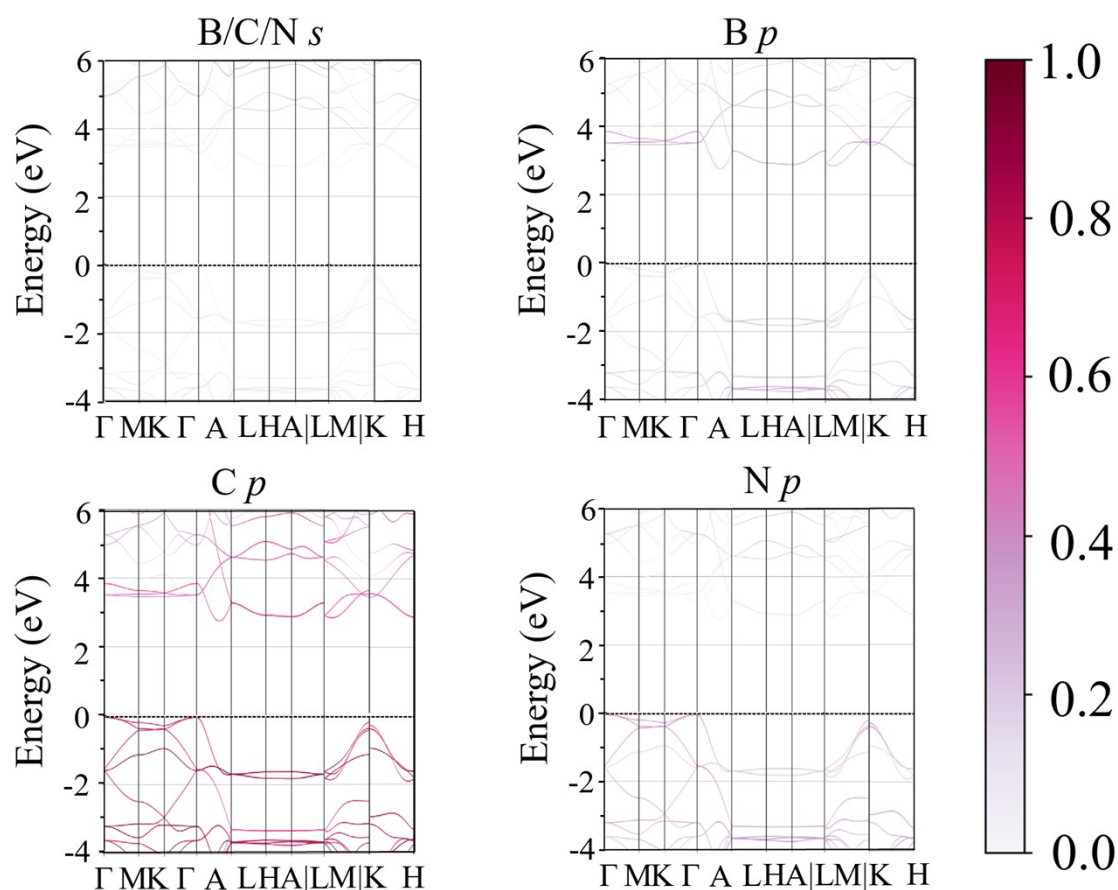


Figure S1. Fatband analysis of PH-BCN.

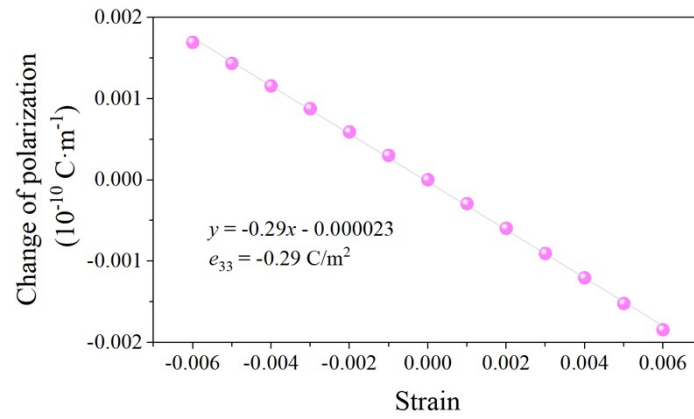


Figure S2. Changes of the polarizations for PH-BCN with the uniaxial strains between -0.6% and 0.6% , giving the value of e_{33} via linear fitting.

Table S1. Changes of the polarizations for PH-BCN with the uniaxial strains between -0.6% and 0.6% .

Strain (%)	Changes of the polarizations ($10^{-13} \text{ C} \cdot \text{m}^{-1}$)
-0.6	1.69
-0.5	1.43
-0.4	1.16
-0.3	0.88
-0.2	0.59
-0.1	0.30
0.0	0.00
0.1	-0.29
0.2	-0.60
0.3	-0.90
0.4	-1.20
0.5	-1.52
0.6	-1.84

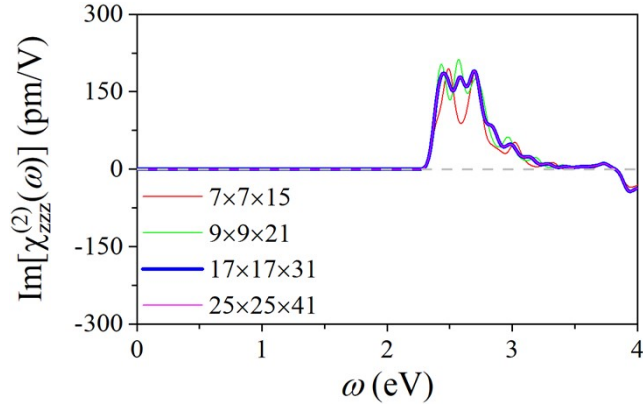


Figure S3. Imaginary part $\text{Im}[\chi^{(2)} zzz(\omega)]$ of the SHG susceptibility of PH-BCN obtained with different k -mesh.

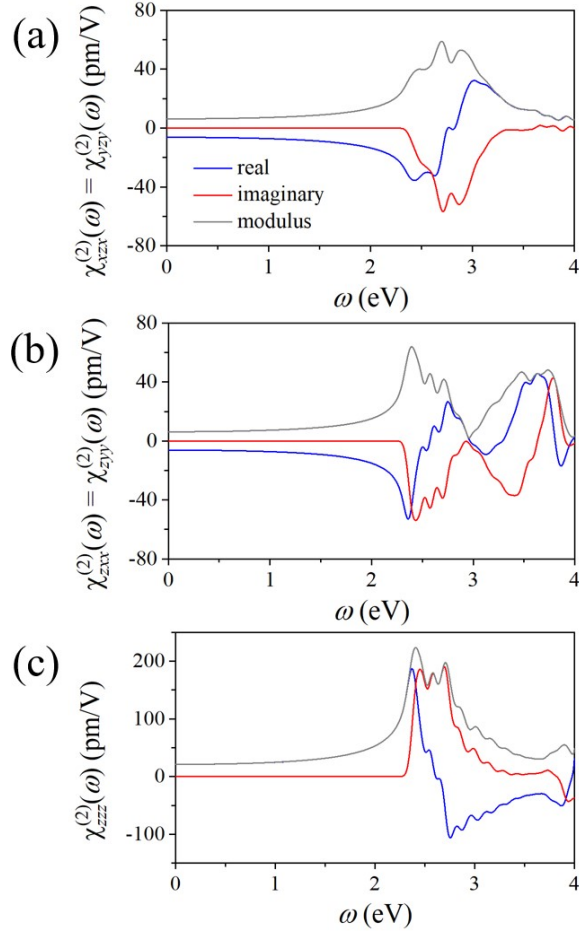


Figure S4. SHG susceptibility (a) $\chi^{(2)} xzx(\omega) = \chi^{(2)} yzy(\omega)$, (b) $\chi^{(2)} zxx(\omega) = \chi^{(2)} zyy(\omega)$, and (c) $\chi^{(2)} zzz(\omega)$ of PH-BCN.

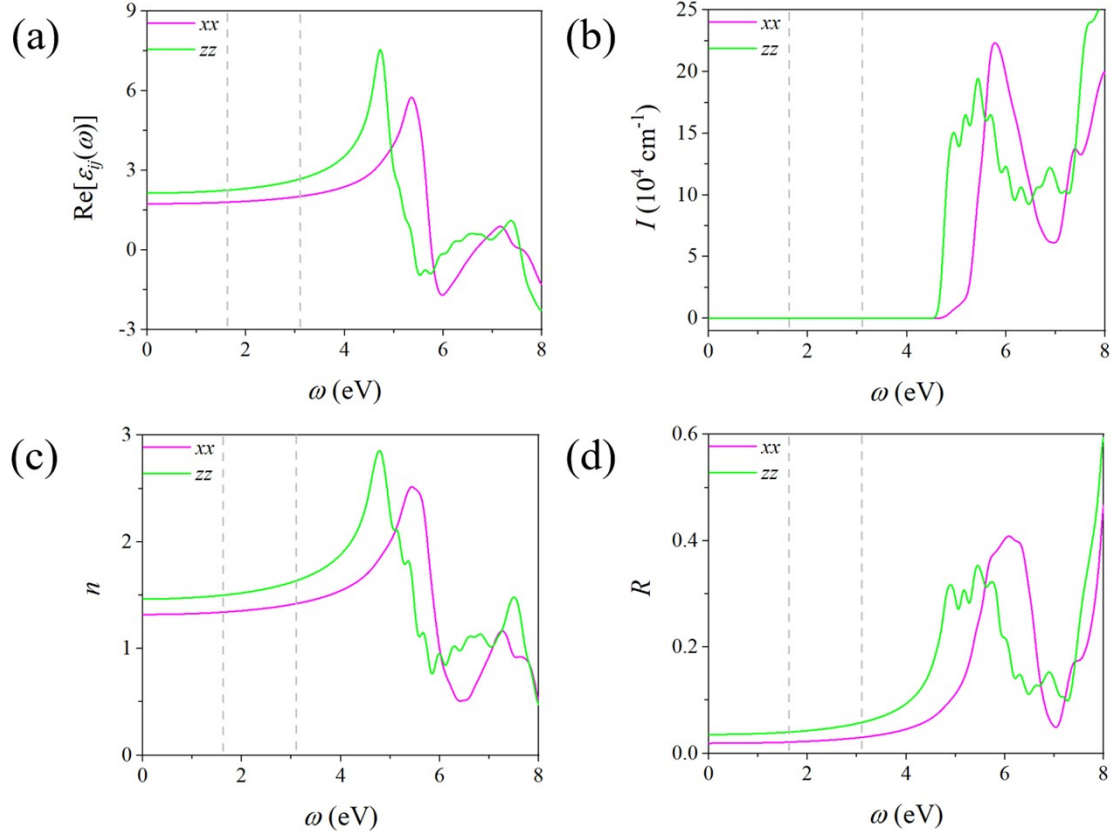


Figure S5. (a) Real part of the dielectric function $\varepsilon_{ij}(\omega)$, (b) absorption coefficient I , (c) refractive index n , (d) reflectivity R of PH-BCN. The visible region of light is denoted by the two dashed lines.

All linear optical properties are determined by the complex dielectric function

$\varepsilon_{ij}(\omega) = \text{Re}[\varepsilon_{ij}(\omega)] + i\text{Im}[\varepsilon_{ij}(\omega)]$,¹ that is the absorption coefficient

$$I(\omega) = \sqrt{2}\omega[\sqrt{[\text{Re}[\varepsilon_{ij}(\omega)]^2 + [\text{Im}[\varepsilon_{ij}(\omega)]^2]} - \text{Re}[\varepsilon_{ij}(\omega)]]^{1/2}, \quad (1)$$

the refractive index

$$n(\omega) = \frac{\sqrt{2}}{2}[\sqrt{[\text{Re}[\varepsilon_{ij}(\omega)]^2 + [\text{Im}[\varepsilon_{ij}(\omega)]^2]} + \text{Re}[\varepsilon_{ij}(\omega)]]^{1/2}, \quad (2)$$

and the reflectivity

$$R(\omega) = \left| \frac{\varepsilon_{ij}(\omega)^{1/2} - 1}{\varepsilon_{ij}(\omega)^{1/2} + 1} \right|^2. \quad (3)$$

Considering the anisotropy of PH-BCN, we separately calculate these parameters along the xx and zz directions. We only consider frequencies lower than 8 eV because they approximately cover the visible spectra. We divide this part into three regions: infrared region (IR) (0-1.63 eV), visible region (VIS) (1.63-3.10 eV), and ultraviolet region (UV) (3.10-8.00 eV). As illustrated in Figure 6(d-e), $\text{Im}[\varepsilon_{ij}(\omega)]$ has negligible value for photons with energy less than ~ 4.5 eV, indicating that little transition can occur under such stimulation. The $\text{Im}[\varepsilon_{ij}(\omega)]$ curve shows two peaks at around 5.80 eV and 4.90 eV for the xx and zz directions, respectively, which can be well explained by the onsets of DOS. The two peaks in the range of 4.90-5.80 eV are mainly attributed to the transitions between C-N valence bands to B-C conduction bands. As shown in Figure S5(b), the absorption coefficient $I(\omega)$ has no value in the infrared and visible regions, indicating that no transition can occur under such stimulation and PH-BCN is a completely transparent. At the same time, $I(\omega)$ shows a significant anisotropy in UV region, indicating that PH-BCN is a promising polarization filter in the UV region. Figure S5(c) shows the refraction index of PH-BCN displays high anisotropy, and the refraction index in the zz direction is larger than that of the xx direction in the range of 0.00-5.12 eV. Figure S5(d) illustrates remarkable increase in the reflectivity within the UV region of light, indicating the significant dispersion. The transparency of PH-BCN along with its anisotropic optical properties, significant absorption, and reflection in the UV region of light indicate the potential application as wave plate, polarization sensitive devices, and coating materials for protection against UV luminance.

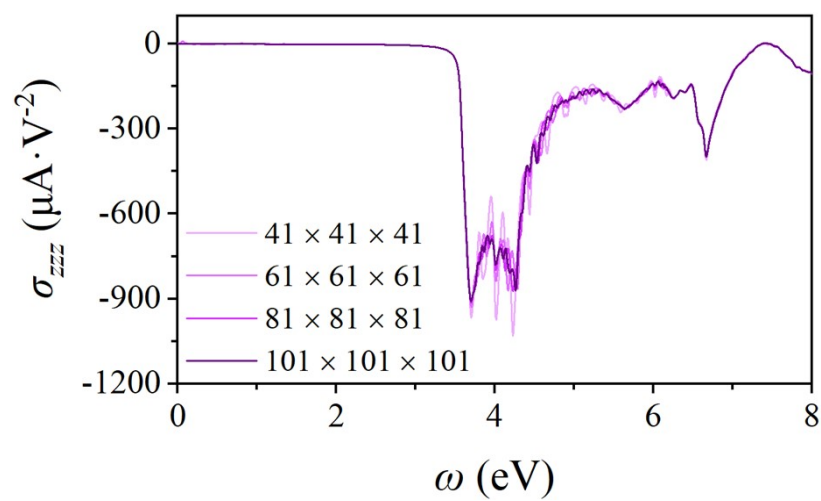


Figure S6. Shift current tensor σ_{zzz} for PH-BCN obtained with different k -mesh.

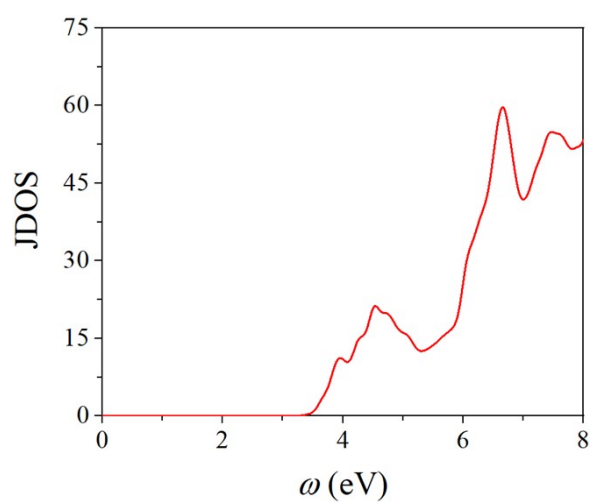


Figure S7. Joint density of states (JDOS) of PH-BCN.

References

- 1 Y. Li, X. Zhao, W. Fan, *J. Phys. Chem. C* **2011**, *115*, 3552.